Salinization and Freshwater–Saline Interface Dynamics Near Underground Energy Storage Sites: A Hydrogeophysical and Machine-Learning-Integrated Review

Raymond Aderoju[1*]; Olanrewaju Ayodele[2]; Moses Falowo[3]; Olaniyi Anisere[4]

[1]Department of Geology, University of Georgia, Georgia, USA
[2]Department of Engineering and Computing Systems, Pennsylvania State University, Harrisburg, USA
[3]Department of Geology, Kansas State University, Kansas, USA
[4]Department of Geology and Geophysics, Louisiana State University, Louisiana, USA

Corresponding Author: Raymond Aderoju[1*]

Publication Date: 2026/09/08

Abstract: Subsurface energy storage, encompassing geological CO_2 sequestration, underground hydrogen storage (UHS), aquifer thermal energy storage (ATES), and compressed-air energy storage (CAES), is expanding rapidly as decarbonization infrastructure, and much of it is sited in or beneath saline formations that directly overlie or adjoin freshwater aquifers. This review synthesizes evidence on an under-recognized consequence of this expansion: storage-induced disturbance of the freshwater–saline interface and consequent salinization risk to overlying underground sources of drinking water (USDW). We identify three principal mechanisms: injection-driven brine displacement and pressure propagation (CO_2/H_2 storage), thermally driven density convection and mixing of a stratified groundwater quality gradient (ATES), and cavern-wall dissolution or well-integrity leakage (CAES/salt-cavern storage). We then derive the governing physics for each from established radial-diffusivity, Rayleigh-number, and Darcy-flow formulations. We evaluate the hydrogeophysical (VES, ERT, TEM, borehole logging, InSAR) and hydrogeochemical (Ghyben–Herzberg-based interface estimation, GALDIT, ionic-ratio diagnostics) methods used to detect these mechanisms, propose a reformulated storage-specific vulnerability index (GALDIT-Storage), and synthesize documented field evidence from Sleipner, In Salah, and Weyburn (the classic megatonne-scale CO_2 storage comparison set), the Otway, Frio, ZERT-Bozeman, and Decatur CO_2 sites, the Farnsworth risk assessment, the Flanders ATES record, and the Huntorf/McIntosh/Pittsfield CAES record. We further examine the integration of machine learning into resistivity inversion, intrusion-extent prediction, and index automation. A recurring finding is that detection methodology is markedly more mature than its storage-specific application, and that documented field evidence, while real and informative, remains concentrated in a handful of instrumented CO_2 and ATES sites; CAES and UHS are comparatively under-documented from a groundwater-monitoring standpoint. We close with a proposed five-stage monitoring framework and near-, medium-, and long-term research priorities.

Keywords: *Storage-Induced Salinization; Underground Energy Storage; Hydrogeophysics; GALDIT Vulnerability Index; Machine Learning; Groundwater Protection.*

How to Cite: Raymond Aderoju; Olanrewaju Ayodele; Moses Falowo; Olaniyi Anisere (2026) Salinization and Freshwater–Saline Interface Dynamics Near Underground Energy Storage Sites: A Hydrogeophysical and Machine-Learning-Integrated Review. *International Journal of Innovative Science and Research Technology*, 11(8), 3027-3037. https://doi.org/10.38124/ijisrt/26aug1167

I. INTRODUCTION

The transition to a low-carbon energy system depends on the ability to store large volumes of gas, air, and heat underground. Geological CO_2 storage and underground hydrogen storage in deep saline aquifers are central to national decarbonization roadmaps [1,2]. Aquifer thermal energy storage is scaling rapidly for seasonal heating and cooling in Europe and compressed-air energy storage in salt caverns and porous aquifers is being revisited as a grid-balancing technology for intermittent renewables. Across all four technologies, the storage target is frequently a saline formation, chosen precisely because its water has no potable value, and that lies in hydraulic communication, however

ISSN No:-2456-2165 https://doi.org/10.38124/ijisrt/26aug1167

indirect, with an overlying or laterally adjacent freshwater aquifer.

This raises a groundwater-protection question that is conceptually distinct from, yet mechanistically related to, the classical problem of coastal seawater intrusion. In coastal aquifers, the freshwater–saline interface is a natural boundary disturbed primarily by abstraction and sea-level rise, as comprehensively synthesized by Werner and colleagues [3]. Storage-induced salinization instead arises from an engineered perturbation, such as injection pressure, thermal cycling, or cavern-wall dissolution, applied to a freshwater–saline boundary that may be deep, laterally extensive, or absent from routine water-quality monitoring networks. Lemieux [4] was among the first to frame this systematically for CO_2 storage, distinguishing a near-field impact from upward-migrating free-phase CO_2 and a far-field impact from the large-scale lateral and vertical displacement of native formation brine as the injected volume seeks space in the reservoir.

The scale of the far-field concern is not hypothetical, and it is best illustrated by the handful of megatonne-scale CO_2 storage projects with the longest monitoring records. At Sleipner (Norway), industrial-scale injection into the Utsira Sand since 1996 has been accompanied by direct pressure measurement in the saline aquifer itself, providing one of the only field-calibrated tests of the pressure-propagation physics in Section 3.1 [18]. At In Salah (Algeria), almost 4 million tonnes of CO_2 were injected between 2004 and 2011 through a 950-m-thick caprock; InSAR and microseismic monitoring detected deformation and probable fluid migration into the lower caprock, yet explicit shallow-aquifer monitoring at the site found no water-quality degradation over the same period [46,47]. Comparative geomechanical analysis across Sleipner, Weyburn (Canada), and In Salah found that the three sites, despite comparable injected volumes, showed markedly different surface-deformation and microseismic responses depending on local fault geometry and stress state, which is direct field evidence that the shared-controls framing in Section 3.4 is not a simplification but the actual governing behavior [46]. Regional-scale simulations of stratified aquifer–aquitard systems show that injection-driven pressure buildup and the native brine it displaces can propagate tens of kilometres from the injection point and interact with overlying formations long before any CO_2 itself arrives [5,6,7]. Deliberate, controlled field experiments, in which CO_2 or CO_2-charged brine was injected directly into or immediately below a shallow freshwater aquifer rather than modeled analytically, provide the most direct evidence available: at the Frio-I Brine Pilot in Texas, 1,600 t of CO_2 injected at 1,500 m depth produced a documented breakthrough at the observation well after 51 hours, with a sharp pH drop and rises in alkalinity, calcium, iron, and manganese, and transient increases in zinc and lead that partially reversed as the system re-equilibrated [9,10]. At the MSU-ZERT controlled-release facility in Bozeman, Montana, food-grade CO_2 was injected 1.5–2.3 m deep directly into a freshwater aquifer with baseline pH of approximately 7 and total dissolved solids of about 600 mg/L; injection produced a rapid, and after cessation largely reversible, drop in pH with increases in conductance, alkalinity, and trace-metal concentrations [11,12,13]. These are process analogues for leakage rather than salinity-specific case studies. Still, they establish, with real measured numbers rather than model output alone, that the geochemical response of a shallow aquifer to a CO_2 or brine perturbation is fast, detectable, and, at least at these test scales, reversible.

Aquifer thermal energy storage introduces a different but related mechanism: cyclic extraction and injection at different depths can homogenize a naturally stratified groundwater quality gradient, altering local salinity and trace-element distributions even where net thermal loading is small [21,22]. Compressed-air and hydrogen storage in salt caverns carry a third, more localized mechanism, cavern-wall dissolution and casing or cement-seal degradation, that can introduce a concentrated brine or dissolution front into groundwater immediately surrounding the storage structure [25,26].

Despite this mechanistic diversity, the methods used to detect and characterize storage-induced salinization are, for the most part, borrowed wholesale from the coastal seawater-intrusion literature: electrical resistivity tomography (ERT), vertical electrical sounding (VES), hydrochemical indices such as GALDIT, and, increasingly, machine-learning-assisted inversion and prediction. This review explicitly connects these detection methods to the storage-specific mechanisms, timescales, and monitoring geometries described above, derives the governing physics for each mechanism from first principles, proposes a storage-adapted reformulation of GALDIT, and compiles the strongest available documented field evidence, including a 2024 regulatory finding at a commercial CO_2 storage site that is directly relevant to USDW protection [16,17,18,19,20]. We ask three questions. RQ1: What physical mechanisms, expressed quantitatively, link subsurface energy storage operations to freshwater–saline interface disturbance, and how do they differ across storage types? RQ2: Which hydrogeophysical, hydrogeochemical, and machine-learning methods have documented capability to detect these mechanisms, and at what maturity? RQ3: Where are the highest-leverage gaps between the coastal-intrusion toolkit as it exists today and what storage-induced salinization monitoring requires?

II. REVIEW METHODOLOGY

➢ *Search Strategy and Scope*

Candidate literature was identified through Scopus, Web of Science, ScienceDirect, PubMed, OSTI.gov, and Google Scholar, combining storage-technology keywords (“CO2 storage”, “underground hydrogen storage”, “aquifer thermal energy storage”, “compressed air energy storage”, “salt cavern”) with groundwater and detection keywords (“salinization”, “seawater intrusion”, “freshwater–saline interface”, “electrical resistivity tomography”, “GALDIT”, “machine learning”, “USDW”). Named-site searches were run explicitly for Sleipner, In Salah, Decatur, Weyburn, Otway, Frio, ZERT-Bozeman, Farnsworth, Huntorf, McIntosh, and Teesside to capture documented field evidence

ISSN No:-2456-2165 https://doi.org/10.38124/ijisrt/26aug1167

rather than relying on general keyword recall. Reference-list snowballing on key reviews [3,8] supplemented the database search. The search window covered January 1967 (for the foundational density-driven flow literature) through July 2026.

- *Inclusion, Quality Screening, and Citation Verification*

Records were included if they reported a quantitative finding or documented methodology relevant to (i) storage-induced pressure, thermal, or chemical perturbation of an overlying or adjacent freshwater–saline boundary, or (ii) a hydrogeophysical, hydrogeochemical, or machine-learning method with demonstrated or plausible application to that problem. Coastal seawater-intrusion studies were included selectively, as methodological analogues, where they establish a detection technique's capability rather than as storage-specific evidence. Screening followed a PRISMA-style flow (Fig. 1) with a quality gate adapted from the Scale for the Assessment of Narrative Review Articles (SANRA) [43], consistent with the reporting approach used in our prior storage- and geochemistry-focused reviews. Every reference retained for synthesis was checked against two criteria before inclusion: the source is retrievable through a DOI, PubMed/PMC identifier, or stable government/institutional record, and its actual subject matter supports the specific claim it is cited for. Numeric values quoted from field studies in Sections 3 and 7 (e.g., breakthrough times, concentration changes, leakage rates) are reproduced only where they appear explicitly in the cited source; where the published record does not report a value for a named site, that gap is stated directly in the text rather than estimated.

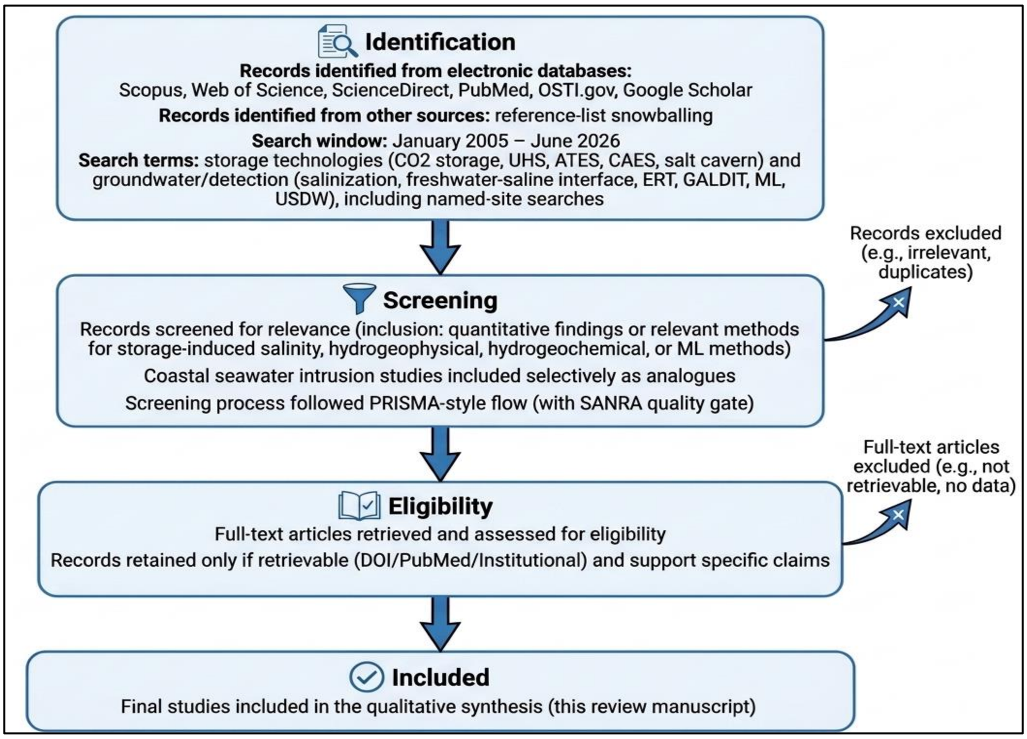

Fig 1 PRISMA-Style Flow Diagram for the Storage-Induced Salinization Review. Search Window: January 2005–June 2026, Adapted from the PRISMA 2020 Flow-Diagram Convention for a Narrative/Critical Review.

III. MECHANISMS OF STORAGE-INDUCED SALINIZATION

- *CO_2 and H_2 Storage: Pressure Propagation and Brine Displacement*

Injection into a saline aquifer raises pore pressure and displaces native brine both laterally, away from the injection point, and, where a leakage pathway such as a permeable fault, fracture, or improperly abandoned well exists, vertically toward shallower formations [4,6,7]. Far-field pressure propagation in a laterally extensive, confined aquifer can be approximated with the radial diffusivity equation used throughout well-hydraulics and reservoir engineering:

$$\partial p/\partial t = (T/S) \cdot (1/r) \cdot \partial/\partial r \, (r \cdot \partial p/\partial r) \qquad (1)$$

Where p is pore pressure (Pa), t is time (s), r is radial distance from the injection well (m), T is aquifer transmissivity (m^2/s), and S is storativity (dimensionless). Multilayered-aquifer solutions built on this formulation show that diffuse leakage through intervening aquitards can transmit the pressure signal into overlying units well before any direct gas contact occurs, and that the transmitted brine volume, not just pressure, is what ultimately determines far-field chemical impact [6,7]. The distinction between near-field impact (upward migration of free-phase gas) and far-field impact (pressure- and brine-driven, potentially reaching a USDW without any CO_2 present at all) is the central organizing idea of this section [4].

Where displaced brine or CO_2-charged fluid reaches a shallow USDW, the dominant early observable is frequently a shift in pH, alkalinity, and major-ion chemistry rather than

ISSN No:-2456-2165 https://doi.org/10.38124/ijisrt/26aug1167

the injected gas itself, sometimes accompanied by trace-metal mobilization governed by the mineralogy of the receiving aquifer and caprock [8,16]. The Illinois Basin–Decatur Project (IBDP) provides the clearest documented illustration to date of this pathway operating outside a controlled experiment: in 2024, the U.S. EPA found that Archer Daniels Midland's Class VI injection well had violated its Safe Drinking Water Act permit after injected fluid migrated into an unauthorized zone roughly 5,000 ft below ground, still separated from the shallow USDW at approximately 200 ft by multiple aquitards. EPA reported no evidence of an actual drinking-water threat, but the incident is the first regulatory-grade confirmation that pressure- and fluid-migration pathways modeled analytically in Section 3.1 do occur at commercial scale [16,17,18]. By contrast, 15 years of hydrochemical monitoring at the Otway International Test Centre in Australia found shallow groundwater quality stable across three CO_2 injection phases, with a 2023 conductivity anomaly at two piezometers attributed to natural seasonal processes rather than the injection program, illustrating that far-field impact is a real but site-specific and not universal outcome [19]. Underground hydrogen storage in saline aquifers shares this brine-displacement mechanism structurally, though hydrogen's lower viscosity and density relative to CO_2 and native brine change the displacement geometry, and near-well salt precipitation from evaporative drying can further modify local porosity and flow paths [26,29].

- *Aquifer Thermal Energy Storage: Thermally Driven Density Convection and Stratification Loss*

ATES systems extract groundwater from one depth, exchange heat, and reinject it at another, cycling seasonally between heating and cooling modes. Two distinct physical mechanisms are conflated in casual discussion of ATES water-quality impact, and separating them matters for monitoring design. The first is advective mixing: cyclic pumping forces water from different depths, and therefore different natural chemical facies, into contact. The second is buoyancy-driven density convection, in which a thermal (or, equivalently, a salinity) contrast across a horizontal interface becomes gravitationally unstable and generates convective fingering rather than simple diffusive mixing. The onset and vigor of this instability are governed by the dimensionless Rayleigh number,

$$Ra = (\Delta\rho \cdot g \cdot k \cdot H) / (\varphi \cdot \mu \cdot D) \quad (2)$$

Where $\Delta\rho$ is the density contrast between the two fluids (kg/m³), g is gravitational acceleration (m/s²), k is intrinsic permeability (m²), H is the characteristic layer thickness (m), φ is porosity, μ is dynamic viscosity (Pa·s), and D is the effective diffusion/dispersion coefficient (m²/s). This formulation, and the associated benchmark problems used to verify numerical codes against it, derive from Elder's original free-convection experiments [41] and were formalized into the variable-density-flow framework used throughout the coastal-intrusion and geothermal literature by Diersch and Kolditz [42]. For thermally driven ATES convection specifically, $\Delta\rho$ is generated by the temperature contrast between injected and ambient groundwater via the thermal expansion coefficient of water rather than by a salinity contrast directly, but the governing balance is structurally identical, which is why the same Rayleigh-number diagnostic applies to both the classical coastal saltwater-upconing problem and the ATES thermal-mixing problem. Field investigations across seven ATES systems in Flanders, Belgium, compared against 69 ambient monitoring wells, found that the imposed temperature differences typical of low-temperature ATES operation ($\Delta T \leq 10$ °C) are too small to drive strong convective instability on their own, and that the dominant observed effect is instead the simpler advective mixing of a naturally stratified vertical water-quality gradient forced by cyclic pumping [21,22]. Laboratory and field work by Bonte and colleagues corroborates this: modelling that combines advective mixing of a stratified aquifer with the observed monitoring data reproduces the measured changes in chemistry without requiring a separate convective term [21]. Where ATES systems operate at higher temperature differentials, or where the natural density gradient is steeper, the Rayleigh-number criterion above indicates convective mixing becomes progressively more important and advective-only models will under-predict the disturbed volume.

- *CAES and Salt-Cavern Storage: Cavern-Wall Dissolution and Pressure-Cycling Leakage*

Compressed air and hydrogen storage in bedded or domal salt caverns depends on salt's low intrinsic permeability for containment. The corresponding salinization risk is comparatively localized but potentially acute: cavern-wall dissolution during leaching and operation, or degradation of the well casing and cement seal, can introduce a concentrated brine or dissolution front into groundwater immediately surrounding the storage structure. Unlike CO_2 or ATES storage, CAES imposes a diurnal-to-weekly pressure cycle rather than a quasi-continuous injection. The cavern pressure at any time can be approximated by a simple polytropic gas relation coupled to the wellbore flow rate, with the cyclic pressure amplitude (typically 43–74 bar across the two operating commercial plants) governing the fatigue loading on the casing-cement-rock interface where leakage pathways originate [25]. The two existing commercial CAES plants, Huntorf (Germany, operating since 1978) and McIntosh (Alabama, USA, operating since 1991), both use solution-mined salt caverns and have operated for decades without a documented groundwater incident, which is informative but should not be over-read: neither plant's public record includes a dedicated, published groundwater-monitoring program comparable to the CO_2-storage sites discussed in Section 3.1 [25]. The most directly relevant historical field data for aquifer-hosted (rather than cavern-hosted) compressed-air storage comes from a 1980s U.S. Department of Energy pilot air-injection test at Pittsfield, Illinois, which confirmed that an air bubble could be created and withdrawn from a porous aquifer at rates feasible for energy recovery, but also documented unexpected heat loss to the formation through the wellbore and oxygen loss from the stored air attributed to oxidation reactions with aquifer minerals and microbial activity, a geochemical interaction pathway with a plausible, though not directly measured in that trial, link to local groundwater chemistry. Where CAES

ISSN No:-2456-2165 https://doi.org/10.38124/ijisrt/26aug1167

is sited in a porous aquifer rather than a cavern (CAES-in-aquifer, CAESA), the displacement mechanism converges structurally with Section 3.1, with the added complication of sub-daily injection–withdrawal cycling rather than the effectively continuous injection typical of CO_2 storage [25].

➢ *Cross-Formational Pathways and Shared Controls*

Across all three mechanisms, three shared controls determine whether a subsurface perturbation actually reaches a freshwater resource: the presence and integrity of confining units and wellbores along the vertical path (the parameter that failed, specifically, in the 2024 Decatur incident); the hydraulic and mineralogical properties of any receiving aquifer, which govern whether displaced or mixed brine is diluted, retarded, or concentrated; and the timescale of storage operation relative to the timescale of natural interface recovery, which the Rayleigh-number and radial-diffusivity formulations above allow to be estimated quantitatively rather than qualitatively. This shared-controls framing is what allows a single hydrogeophysical and hydrogeochemical detection toolkit, discussed next, to be applied meaningfully across otherwise mechanistically distinct storage types.

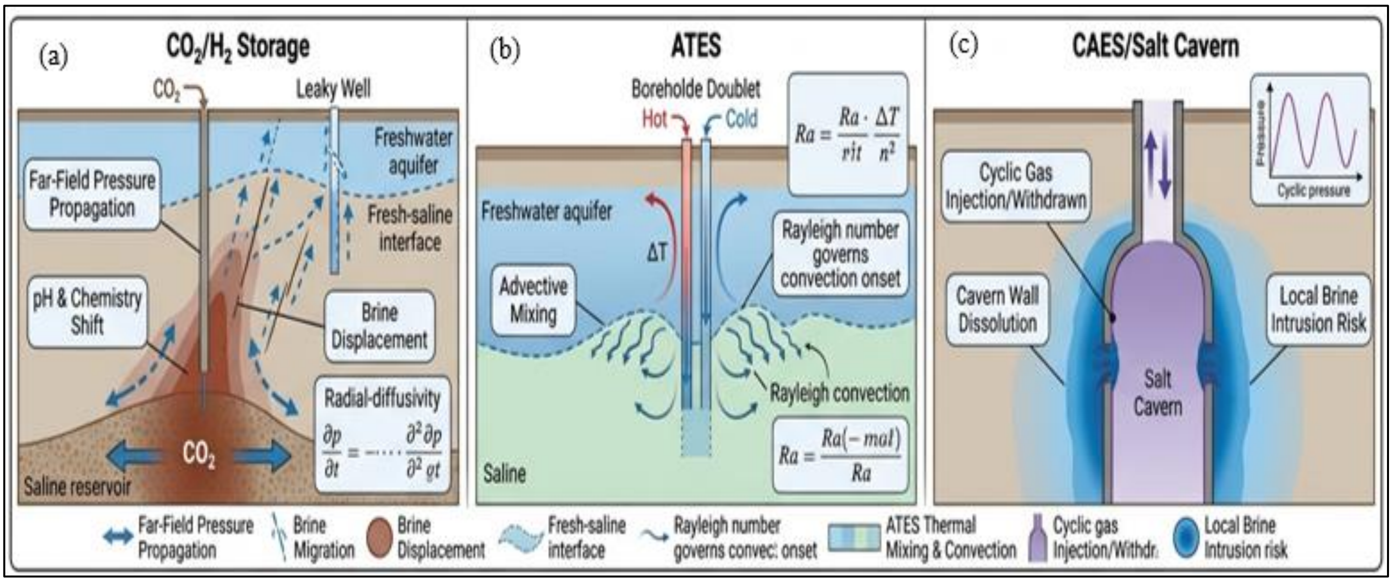

Fig 2 Conceptual Mechanisms of Storage-Induced Salinization of Overlying Freshwater Aquifers. (a) Pore-Pressure Buildup Displaces Native Brine Laterally and, Along Leakage Pathways, Vertically Toward the USDW. (b) Cyclic ATES Pumping Homogenizes a Naturally Stratified Quality Gradient. (c) Cavern-Wall or Well-Integrity Leakage Introduces a Localized High-Salinity Plume Near the Storage Structure.

IV. HYDROGEOPHYSICAL DETECTION METHODS

➢ *Vertical Electrical Sounding and Electrical Resistivity Tomography*

Electrical methods remain the workhorse of freshwater–saline interface characterization because the resistivity contrast between fresh and saline pore water is large and well calibrated against salinity and total dissolved solids. Vertical electrical sounding (VES) provides a low-cost, 1-D point estimate of interface depth and has been used extensively to characterize coastal aquifers structurally similar to the storage-adjacent settings discussed here, including detailed regional work across the Nigerian coastal plain, where Q-type resistivity curves and near-surface resistivities below roughly 10 Ω·m consistently mark the intruded zone at depths of 10–50 m [37]. Electrical resistivity tomography (ERT) extends this to 2-D and 3-D profiling and, critically for storage applications, supports repeat time-lapse surveying, which is what distinguishes a static natural interface from an evolving, storage-induced one. Machine-learning-based forward operators embedded in probabilistic ERT inversion schemes now allow this time-lapse workflow to be run at a fraction of the computational cost of conventional finite-element inversion while retaining comparable uncertainty quantification [40].

➢ *Time-Domain Electromagnetic Methods*

Time-domain electromagnetic (TEM/TDEM) surveying trades some of ERT's spatial resolution for substantially greater areal coverage and depth penetration, making it a natural complement for the regional-scale pressure and brine-displacement footprint associated with CO_2 and H_2 storage (Section 3.1), where the area of concern, as the radial-diffusivity equation in Section 3.1 makes explicit, can extend well beyond what a ground-based electrode array can practically cover.

➢ *Borehole Geophysical Logging*

Borehole electrical-conductivity and temperature logging provides the highest-fidelity, if spatially limited, record of interface position and is the natural fit for the depth-stratified mixing problem of ATES (Section 3.2), where the vertical quality gradient itself, not just its lateral extent, is the object of concern. This is also the method class used in every documented CO_2-brine field test discussed in Section 7 (Frio, ZERT-Bozeman, Otway), underscoring that borehole sampling, not surface geophysics, remains the actual evidentiary backbone of the field record to date.

ISSN No:-2456-2165 https://doi.org/10.38124/ijisrt/26aug1167

➢ *InSAR and Surface Deformation Monitoring*

Satellite InSAR does not directly image salinity but detects the surface deformation that can accompany pressure buildup, brine displacement, or cavern-volume change at depth, providing a regional early-warning signal that can be used to target more resolving ground-based surveys.

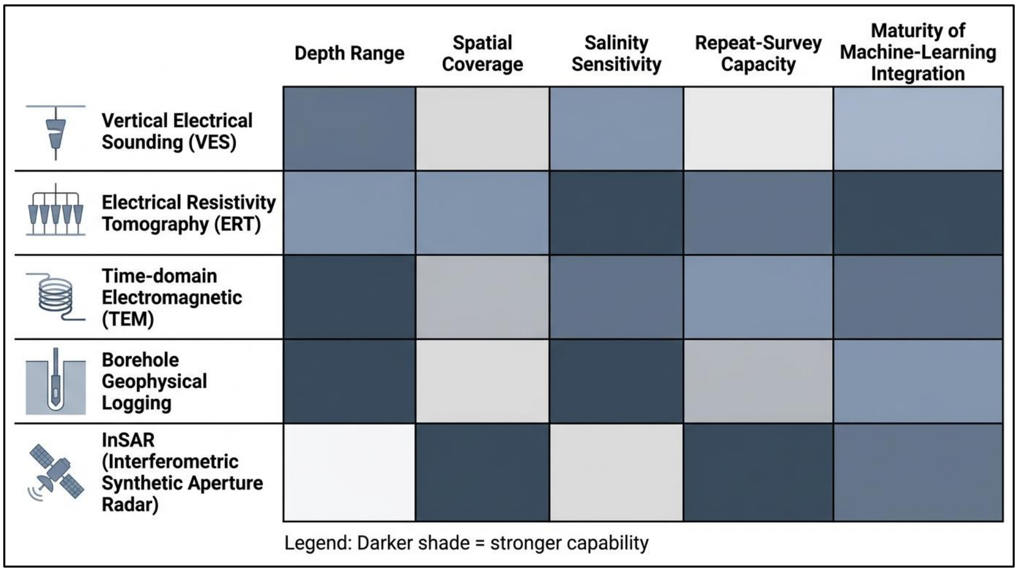

Fig 3 Capability Matrix Comparing Detection Methods Against Depth Range, Spatial Coverage, Salinity Sensitivity, Repeat-Survey Capacity, and Current Maturity of Machine-Learning Integration. Darker Shading Indicates Relatively Stronger Performance for that Column.

➢ *Hydrogeochemical Indices and Diagnostics*

- *Interface-Position Estimation*

The classical Ghyben–Herzberg relation [35,36], relating freshwater lens thickness to the height of the water table above sea level under sharp-interface, static-equilibrium assumptions, remains the conceptual starting point for estimating interface position analytically, even though its assumptions are violated by the transient, pressure- or thermally-driven perturbations characteristic of energy storage discussed in Section 3.

- *Toward a Storage-Adapted Vulnerability Index: GALDIT-Storage*

The GALDIT method, developed by Chachadi and Lobo-Ferreira [34], combines six weighted hydrogeological parameters (Groundwater occurrence, Aquifer hydraulic conductivity, height of groundwater Level above sea level, Distance from the shore, Impact of existing seawater intrusion, and aquifer Thickness) into a single vulnerability index within a GIS framework, originally for coastal seawater intrusion. We propose here, as an original methodological contribution of this review rather than a synthesis of prior published work, a re-specification of each GALDIT parameter for the storage-induced setting, which we term GALDIT-Storage (GS). The re-specification retains the original multiplicative weighted-sum structure.

$$GS = \Sigma_i (W_i \cdot R_i) / \Sigma_i W_i , \ \ i = 1 \qquad (3)$$

Where W_i is the fixed importance weight of parameter i (retained at GALDIT's original values: G=1, A=3, L=4, D=4, I=1, T=2, on a 1–10 scale) and R_i is the site-specific rating (1–10) of that parameter. The re-specification changes only what each parameter measures, not the arithmetic:

- ✓ G (storage-zone Groundwater occurrence): rated by the confined/unconfined character and vertical connectivity of the receiving aquifer above the storage zone, rather than the coastal aquifer type in the original formulation.
- ✓ A (Aquifer hydraulic conductivity): retained directly from GALDIT, since it governs both natural intrusion and storage-induced brine transport identically.
- ✓ L (pressure-equivalent groundwater Level): re-specified as the modeled or monitored excess pore pressure at the base of the receiving aquifer, non-dimensionalized against native hydrostatic pressure, in place of the original static water-table height above sea level. This directly links the parameter to the radial-diffusivity solution of Section 3.1.
- ✓ D (Distance): re-specified as the 3-D slant distance from the injection well, cavern, or ATES well-doublet, rather than horizontal distance from a coastline.
- ✓ I (Impact of existing intrusion): re-specified as evidence of an already-measurable storage-related chemistry shift at a monitoring well (e.g., the pH, alkalinity, or trace-metal excursions documented in Section 3.1 and Section 7), in place of existing seawater-intrusion evidence.
- ✓ T (aquifer Thickness): retained directly, since thinner receiving aquifers concentrate a given intruded volume into a larger relative salinity change.

This reformulation is presented as a testable proposal, not a validated instrument: it has not, to our knowledge, been applied to any documented site, and its first validation should compare GS classifications against the documented field responses compiled in Section 7, for example by testing whether the Decatur incident (Section 3.1) and the null result

ISSN No:-2456-2165 https://doi.org/10.38124/ijisrt/26aug1167

at Otway (Section 3.1) receive appropriately different GS scores under a consistent rating protocol. We identify this validation explicitly as a near-term research priority in Section 9 rather than claiming it here.

- *Ionic Ratios and Hydrochemical Facies*

Beyond total dissolved solids and chloride concentration, ionic ratios (Na^+/Cl^-, Ca^{2+}/Mg^{2+}, base-exchange indices) and Piper- or Gibbs-diagram facies classification provide a complementary, process-level diagnostic: they can distinguish a genuine brine-mixing or displacement signal from confounding sources such as agricultural or urban contamination. The Frio-I and ZERT-Bozeman field tests summarized in Section 7 are, to date, the clearest demonstrations that alkalinity, Ca, Fe, and Mn respond faster and more diagnostically to a CO_2-brine perturbation than chloride or TDS alone [9,11], a finding with direct implications for which ions a storage-adjacent monitoring program should prioritize.

➢ *Machine Learning Integration*

Machine learning enters the storage-induced salinization problem at three points, mirroring its role in the broader groundwater-quality modelling literature [38,39].

- *ML-Assisted Geophysical Inversion*

Deep-learning approaches to ERT inversion, including convolutional and residual-network architectures and machine-learning-based forward operators embedded in probabilistic (Bayesian) inversion schemes [40], can reduce the computational cost of inversion by orders of magnitude relative to conventional finite-element forward modelling, while retaining comparable uncertainty quantification. This matters directly for storage-adjacent monitoring, where repeat time-lapse surveys over an operational storage lifetime of decades demand an inversion workflow that is fast enough to run routinely rather than as an occasional research exercise.

- *Prediction of Intrusion and Interface Extent*

Reviews of machine learning and deep learning applied to coastal groundwater salinity modelling document a broad and maturing toolkit, including gradient-boosted trees, random forests, artificial neural networks, and Bayesian model-averaging ensembles, for predicting intrusion wedge length, salinity distribution, and vulnerability class from hydrochemical and hydrogeological features [38,39]. None of this literature, to our knowledge, has yet been retrained or validated against a documented energy-storage-induced salinization dataset rather than a natural coastal-intrusion one; the Otway, Frio, and ZERT-Bozeman datasets summarized in Section 7 are, to our knowledge, the first candidates for such a retraining exercise, though none was collected with that use explicitly in mind.

- *Automated Index Computation and Uncertainty Quantification*

A more modest but immediately actionable application is the automation of index computation itself: coupling the proposed GALDIT-Storage index (Section 5.2) or ionic-ratio classification directly to a live sensor and geophysical-inversion feed would convert a periodic, manually computed vulnerability snapshot into a continuously updated one, with model uncertainty propagated through to the final index value rather than reported as if the index were exact.

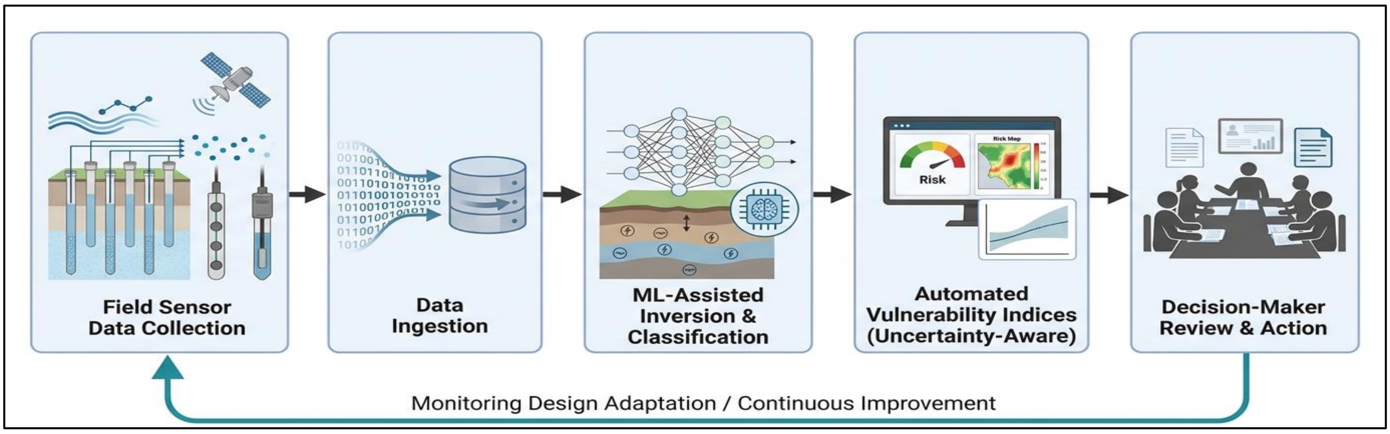

Fig 4 Machine-Learning-in-the-Loop Monitoring Workflow for Storage-Induced Salinization. Field Sensor Data are Ingested, Inverted/Classified with ML-Assisted Methods, Converted into Automated Vulnerability Indices, and Returned to Decision-Makers, who Adapt the Monitoring Design in a Closed Feedback Loop.

V. DOCUMENTED CASE EVIDENCE

This section compiles the strongest available documented evidence, prioritizing sources that report actual measured field data over general technology reviews. Fig. 5 synthesizes eight cases spanning all three storage mechanisms discussed in Section 3. Four of these, namely Frio, ZERT-Bozeman, Otway, and In Salah, are CO_2-specific field programs with monitoring-well data reported directly in the cited sources, and two of the four (Otway, In Salah) are documented null results: extensive shallow-aquifer monitoring at both sites found no water-quality degradation attributable to the injection program, which is itself informative and is stated as such rather than omitted for being a negative finding. The Decatur case is, to our knowledge, the first regulatory-confirmed instance of an injected-fluid migration event at a commercial-scale CO_2 storage project, and is included because it demonstrates that the pressure/brine-migration pathway modeled in Section 3.1 is not purely theoretical, while also illustrating that a migration event and a documented USDW impact are not the same thing: EPA's finding was a permit violation, not a confirmed drinking-water contamination. The Farnsworth case is a quantitative risk model rather than a monitoring record. The Flanders ATES case is the most complete groundwater-quality dataset available for any storage type discussed in this review (69 reference wells). The Huntorf/McIntosh/Pittsfield CAES row is the weakest in direct groundwater evidence and is included specifically to make that evidentiary gap visible rather than to overstate what is known. Sleipner and Weyburn are discussed in Section 3.1 for their pressure and geomechanical monitoring records [18,46] but are not given their own row here, because neither site's public record includes the kind of dedicated shallow-aquifer chemistry monitoring reported for Otway, In Salah, Frio, and ZERT-Bozeman, a gap we consider worth stating plainly rather than filling with an estimated entry.

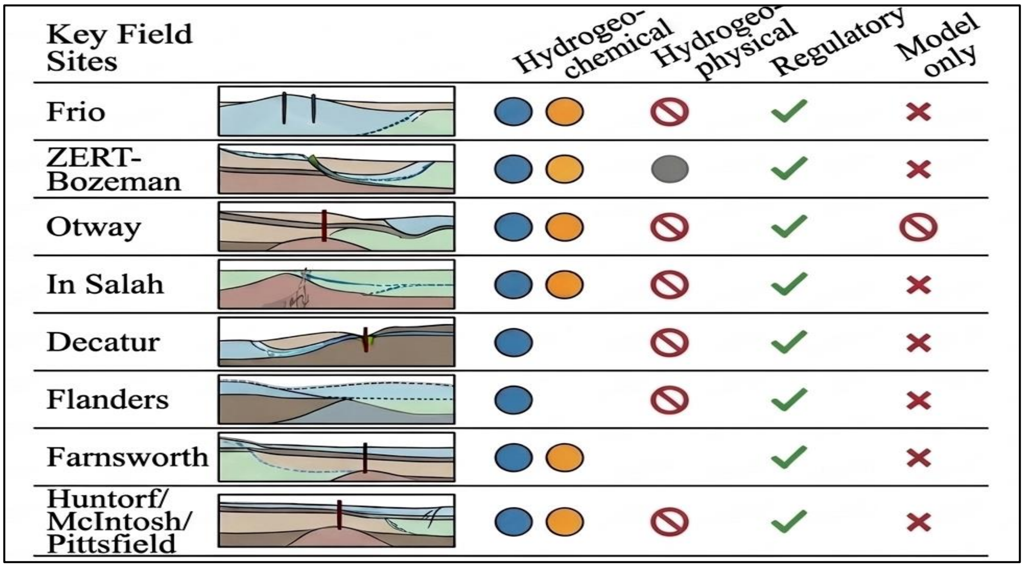

Fig 5 Documented Case Evidence Relevant to Storage-Induced Salinization, Spanning CO_2 Storage, ATES, and CAES. Amber Rows Denote a Regulatory/Incident Record (Decatur) and a Technology-Analogue Field Trial (Pittsfield) Rather than a Routine Monitoring Result.

- *Critical Gaps and a Proposed Monitoring Framework*

Three gaps recur across Sections 3–7. First, detection methodology (Sections 4–5) is markedly more mature than its storage-specific application: ERT, VES, and GALDIT are all well-validated for coastal seawater intrusion but have seen almost no published re-parameterization for storage-induced geometries; the GALDIT-Storage proposal in Section 5.2 is offered as a first, unvalidated step toward closing this gap. Second, the machine-learning literature (Section 6) is built almost entirely on coastal training data; its transfer performance to storage-adjacent settings is untested, even though the Otway, Frio, and ZERT-Bozeman records (Section 7) now provide at least a starting benchmark. Third, and most consequentially, sustained field-monitoring datasets that pair storage operational records directly with repeat hydrogeophysical or hydrochemical surveys of the overlying aquifer are concentrated in a small number of CO_2 sites and one ATES region (Flanders); CAES and UHS are particularly under-documented, as Section 7 makes explicit rather than papering over.

We propose a five-stage monitoring framework, shown in Fig. 4 and summarized here as an operational sequence: (1) baseline characterization of the natural freshwater–saline interface and vertical quality gradient before storage operation begins, using VES/ERT and borehole logging, the step that was evidently in place at Otway and Flanders and that allowed the null and small-effect findings there to be stated with confidence; (2) installation of a repeat-survey network sized to the storage type's characteristic displacement footprint, using the radial-diffusivity (Section 3.1) or Rayleigh-number (Section 3.2) estimate to set the network radius rather than an arbitrary buffer distance; (3) ML-assisted inversion and index computation integrated into routine, not occasional, data processing; (4) explicit uncertainty propagation from raw geophysical signal through to a reported vulnerability class; and (5) an adaptive feedback step in which the monitoring network design itself is revised as the vulnerability estimate and its uncertainty evolve.

- *Roadmap for Future Research*

- Near-term (0–2 years): validate the GALDIT-Storage reformulation (Section 5.2) against the Otway, Frio, ZERT-Bozeman, and Decatur records compiled in Section 7, since these are, to our knowledge, the only documented sites with sufficient published data to attempt this now; mandate baseline pre-operational hydrogeophysical surveys as a permitting condition, extending the Class VI precedent explicitly to ATES and CAES permitting where it does not yet exist.
- Medium-term (3–5 years): build a dedicated, storage-specific machine-learning benchmark dataset from the Flanders ATES record (the most complete dataset identified in this review) and retrain the coastal-intrusion toolkit against it rather than assuming direct transfer;

ISSN No:-2456-2165 https://doi.org/10.38124/ijisrt/26aug1167

commission a groundwater-monitoring program at an operating CAES site (cavern or aquifer) comparable in scope to the CO_2-storage field tests in Section 7, since no such dataset currently exists in the published record.

- Long-term (5–10 years): couple ML-assisted geophysical inversion directly to reservoir-scale pressure and brine-displacement models so that a single, physically consistent workflow spans from the injection well to the overlying USDW, using the radial-diffusivity and Rayleigh-number formulations in Section 3 as the physical backbone; extend systematic field monitoring to UHS sites, none of which currently has a published groundwater-monitoring record comparable to Section 7's CO_2 cases.

VI. CONCLUSION

Subsurface energy storage and freshwater–saline interface science have developed largely in parallel: the storage literature treats groundwater protection chiefly as a leakage and USDW-contamination problem, while the hydrogeophysical and hydrogeochemical literature has refined its detection toolkit almost entirely against the natural, abstraction-driven coastal intrusion problem. This review has shown, using documented field data rather than inference alone, that the mechanisms differ in a way that is now quantifiable: pressure- and brine-driven displacement in CO_2/H_2 storage (Section 3.1, confirmed at commercial scale by the 2024 Decatur incident), thermally driven mixing dominated by advection rather than convective instability at current ATES operating temperatures (Section 3.2, established at Flanders), and localized cavern-integrity leakage in CAES (Section 3.3, the least directly evidenced of the three). The same electrical, electromagnetic, and index-based methods that resolve a coastal freshwater–saline wedge are directly applicable to all three, provided their parameterization and monitoring geometry are adapted to the storage-specific mechanism; the GALDIT-Storage proposal in Section 5.2 is offered as a concrete, testable step in that direction. Machine learning offers a genuine, if still largely unproven in this specific context, route to making that monitoring continuous and uncertainty-aware rather than periodic and point-based. The most consequential single step available to the field is also the least technically demanding: pairing routine storage operational data with routine overlying-aquifer monitoring at a larger number of sites, across all four storage types, so that the mechanism-specific claims made in this review can be tested directly rather than inferred by analogy.

REFERENCES

[1]. Intergovernmental Panel on Climate Change. Climate Change 2022: Mitigation of Climate Change. Working Group III contribution to the Sixth Assessment Report. Cambridge: Cambridge University Press; 2022.

[2]. International Energy Agency. Net Zero by 2050: A Roadmap for the Global Energy Sector. Paris: IEA; 2021.

[3]. Werner AD, Bakker M, Post VEA, Vandenbohede A, Lu C, Ataie-Ashtiani B, Simmons CT, Barry DA. Seawater intrusion processes, investigation and management: recent advances and future challenges. Adv Water Resour. 2013;51:3–26. doi:10.1016/j.advwatres.2012.03.004.

[4]. Lemieux JM. The potential impact of underground geological storage of carbon dioxide in deep saline aquifers on shallow groundwater resources. Hydrogeol J. 2011;19(4):757–778. doi:10.1007/s10040-011-0715-4.

[5]. Celia MA, Bachu S, Nordbotten JM, Bandilla KW. Status of CO2 storage in deep saline aquifers with emphasis on modeling approaches and practical simulations. Water Resour Res. 2015;51(9):6846–6892. doi:10.1002/2015WR017609.

[6]. Birkholzer JT, Zhou Q, Tsang CF. Large-scale impact of CO2 storage in deep saline aquifers: a sensitivity study on the pressure response in stratified systems. Int J Greenh Gas Control. 2009;3(2):181–194.

[7]. Cihan A, Birkholzer JT, Zhou Q. Pressure buildup and brine migration during CO2 storage in multilayered aquifers. Groundwater. 2013;51(2). doi:10.1111/j.1745-6584.2012.00972.x.

[8]. Qafoku NP, Lawter AR, Bacon DH, Zheng L, Kyle J, Brown CF. Review of the impacts of leaking CO2 gas and brine on groundwater quality. Earth-Sci Rev. 2017;169:69–84. doi:10.1016/j.earscirev.2017.04.010.

[9]. Kharaka YK, Cole DR, Hovorka SD, Gunter WD, Knauss KG, Freifeld BM. Gas-water-rock interactions in Frio Formation following CO2 injection: implications for the storage of greenhouse gases in sedimentary basins. Geology. 2006;34(7):577–580. doi:10.1130/G22357.1.

[10]. Kharaka YK, Thordsen JJ, Hovorka SD, Nance HS, Cole DR, Phelps TJ, Knauss KG. Potential environmental issues of CO2 storage in deep saline aquifers: geochemical results from the Frio-I brine pilot test, Texas, USA. Appl Geochem. 2009;24(6):1106–1112.

[11]. Kharaka YK, Thordsen JJ, Kakouros E, Ambats G, Herkelrath WN, Beers SR, Birkholzer JT, Apps JA, Spycher NF, Zheng L, Trautz RC, Rauch HW, Gullickson KS. Changes in the chemistry of shallow groundwater related to the 2008 injection of CO2 at the ZERT field site, Bozeman, Montana. Environ Earth Sci. 2010;60(2):273–284. doi:10.1007/s12665-009-0401-1.

[12]. Spangler LH, Dobeck LM, Repasky KS, Nehrir AR, Humphries SD, Barr JL, Keith CJ, Shaw JA, Rouse JH, Cunningham AB, Benson SM, Oldenburg CM, Lewicki JL, Wells AW, Diehl JR, Strazisar BR, Fessenden JE, Rahn TA, Amonette JE, Barr JL, Pickles WL, Jacobson JD, Silver EA, Male EJ, Rauch HW, Gullickson KS, Trautz RC, Kharaka YK, Birkholzer JT, Wielopolski L. A shallow subsurface controlled release facility in Bozeman, Montana, USA, for testing near surface CO2 detection techniques and transport models. Environ Earth Sci. 2010;60(2):227–239. doi:10.1007/s12665-009-0400-2.

[13]. Apps JA, Zheng L, Spycher N, Birkholzer JT, Kharaka YK, Thordsen JJ, Kakouros E, Trautz RC. Transient

changes in shallow groundwater chemistry during the MSU ZERT CO2 injection experiment. Energy Procedia. 2011;4:3231–3238.

[14]. Xiao T, Dai Z, Viswanathan H, Hakala A, Cather M, Jia W, Zhang Y, McPherson B. Arsenic mobilization in shallow aquifers due to CO2 and brine intrusion from storage reservoirs. Sci Rep. 2017;7(1):2549. doi:10.1038/s41598-017-02849-z.

[15]. Xiao T, McPherson B, Esser R, Jia W, Dai Z, Chu S, Pan F, Viswanathan H. Chemical impacts of potential CO2 and brine leakage on groundwater quality with quantitative risk assessment: a case study of the Farnsworth Unit. Energies. 2020;13(24):6574. doi:10.3390/en13246574.

[16]. Shao H, Freiburg JT, Berger PM, Taylor AH, Cohen HF, Locke RA. Mobilization of trace metals from caprock and formation rocks at the Illinois Basin–Decatur Project demonstration site under geological carbon dioxide sequestration conditions. Chem Geol. 2020;550:119758. doi:10.1016/j.chemgeo.2020.119758.

[17]. Zhou Z, Zhang K, Callahan DL, Timms W. Shallow groundwater near a deep-well CO2 storage site—15 years of stable water quality for agricultural use. Environ Sci Pollut Res. 2025. doi:10.1007/s11356-025-35906-6.

[18]. Chadwick RA, Williams GA, Williams JDO, Noy DJ. Measuring pressure performance of a large saline aquifer during industrial-scale CO2 injection: the Utsira Sand, Norwegian North Sea. Int J Greenh Gas Control. 2012;10:374–388. doi:10.1016/j.ijggc.2012.06.022.

[19]. Kim J, Lee S, Ha S, Joun W, Ju YJ, Lee K. Natural 222Rn as a tracer of mixing and volatilization in a shallow aquifer during a CO2 injection experiment. Hydrol Process. 2020;34(26):5417–5428.

[20]. U.S. Environmental Protection Agency. EPA Announces Proposed Order Requiring Archer Daniels Midland Co. to Take Actions to Ensure Safe Operation of its Carbon Sequestration Well in Decatur, Illinois. Press release. Washington, DC: US EPA; 2024.

[21]. Bonte M, Van Breukelen BM, Stuyfzand PJ. Environmental impacts of aquifer thermal energy storage investigated by field and laboratory experiments. J Water Clim Change. 2013;4(2):77–89.

[22]. Possemiers M, Huysmans M, Batelaan O. Influence of aquifer thermal energy storage on groundwater quality: a review illustrated by seven case studies from Belgium. J Hydrol Reg Stud. 2014;2:20–34. doi:10.1016/j.ejrh.2014.08.001.

[23]. Fleuchaus P, Godschalk B, Stober I, Blum P. Worldwide application of aquifer thermal energy storage - A review. Renew Sustain Energy Rev. 2018;94:861–876.

[24]. Jesußek A, Grandel S, Dahmke A. Impacts of subsurface heat storage on aquifer hydrogeochemistry. Environ Earth Sci. 2013;69:1999–2012. doi:10.1007/s12665-012-2037-9.

[25]. Guo C, Li C, Zhang K, Cai Z, Ma T, Maggi F, Gan Y, El-Zein A, Pan Z, Shen L. The promise and challenges of utility-scale compressed air energy storage in aquifers. Appl Energy. 2021;286:116513. doi:10.1016/j.apenergy.2021.116513.

[26]. Heinemann N, Alcalde J, Miocic JM, Hangx SJT, Kallmeyer J, Ostertag-Henning C, Hassanpouryouzband A, et al. Enabling large-scale hydrogen storage in porous media – the scientific challenges. Energy Environ Sci. 2021;14(2):853–864.

[27]. Zivar D, Kumar S, Foroozesh J. Underground hydrogen storage: a comprehensive review. Int J Hydrogen Energy. 2021;46(45):23436–23462.

[28]. Thaysen EM, McMahon S, Strobel GJ, Butler IB, Ngwenya BT, Heinemann N, Wilkinson M, Hassanpouryouzband A, McDermott CI, Edlmann K. Estimating microbial growth and hydrogen consumption in hydrogen storage in porous media. Renew Sustain Energy Rev. 2021;151:111481. doi:10.1016/j.rser.2021.111481.

[29]. Braid H, Taylor K, Hough E, Rochelle C, Niasar V, Ma L. Hydrogen-induced mineral alteration: a review in the context of underground hydrogen storage (UHS) in saline aquifers. Earth-Sci Rev. 2024;104975. doi:10.1016/j.earscirev.2024.104975

[30]. Borghini L, Corradetti A, Del Ben A, Franceschi M, Bonini L. Underground hydrogen storage suitability index: a geological tool for evaluating and ranking storage sites. Int J Hydrogen Energy. 2025.

[31]. Iranfar S, Sadeghpour F, Shakiba M, Naderi M, Hassanpouryouzband A. Multi-criteria framework for ranking geological sites in underground hydrogen storage. Environ Sci Adv. 2026;5:107–117. doi:10.1039/D5VA00380F.

[32]. Derakhshani R, Lankof L, GhasemiNejad A, Zaresefat M. Artificial intelligence-driven assessment of salt caverns for underground hydrogen storage in Poland. Sci Rep. 2024;14(1):14246. doi:10.1038/s41598-024-64020-9.

[33]. Okoroafor ER, Saltzer SD, Kovscek AR. Toward underground hydrogen storage in porous media: reservoir engineering insights. Int J Hydrogen Energy. 2022;47(79):33781–33802. doi:10.1016/j.ijhydene.2022.07.239.

[34]. Chachadi AG, Lobo-Ferreira JP. Sea water intrusion vulnerability mapping of aquifers using GALDIT method. In: Proceedings of the Workshop on Modelling in Hydrogeology. Chennai: Anna University; 2001. p.143–156.

[35]. Ghijben WB. Nota in verband met de voorgenomen putboring nabij Amsterdam. Tijdschr K Inst Ing. 1888/1889:8–22.

[36]. Herzberg A. Die Wasserversorgung einiger Nordseebader. J Gasbeleucht Wasserversorg. 1901;44:815–819, 842–844.

[37]. Adepelumi AA, Ako BD, Ajayi TR, Afolabi O, Omotoso EJ. Delineation of saltwater intrusion into the freshwater aquifer of Lekki Peninsula, Lagos, Nigeria. Environ Geol. 2008;56(5):927–933. doi:10.1007/s00254-008-1194-3.

[38]. Roy DK, Sarkar TK, Munmun TH, Paul CR, Datta B. A review on the applications of machine learning and deep learning to groundwater salinity modeling: present status, challenges, and future directions.

ISSN No:-2456-2165 https://doi.org/10.38124/ijisrt/26aug1167

Discov Water. 2025;5:16. doi:10.1007/s43832-025-00207-z.
[39]. Haggerty R, Sun J, Yu H, Li Y. Application of machine learning in groundwater quality modeling: a comprehensive review. Water Res. 2023;233:119745. doi:10.1016/j.watres.2023.119745.
[40]. Aleardi M, Vinciguerra A, Stucchi E, Hojat A. Probabilistic inversions of electrical resistivity tomography data with a machine learning-based forward operator. Geophys Prospect. 2022;70(5):938–957.
[41]. Elder JW. Steady free convection in a porous medium heated from below. J Fluid Mech. 1967;27(1):29–48.
[42]. Diersch HJ, Kolditz O. Variable-density flow and transport in porous media: approaches and challenges. Adv Water Resour. 2002;25(8–12):899–944.
[43]. Baethge C, Goldbeck-Wood S, Mertens S. SANRA: a scale for the quality assessment of narrative review articles. Res Integr Peer Rev. 2019;4:5. doi:10.1186/s41073-019-0064-8.
[44]. Page MJ, McKenzie JE, Bossuyt PM, et al. The PRISMA 2020 statement: an updated guideline for reporting systematic reviews. BMJ. 2021;372:n71.
[45]. U.S. Environmental Protection Agency. Federal Requirements Under the Underground Injection Control (UIC) Program for Carbon Dioxide Geologic Sequestration (Class VI) Wells; Final Rule. Fed Regist. 2010;75(237):77230–77303.
[46]. Verdon JP, Kendall JM, Stork AL, Chadwick RA, White DJ, Bissell RC. Comparison of geomechanical deformation induced by megatonne-scale CO2 storage at Sleipner, Weyburn, and In Salah. Proc Natl Acad Sci USA. 2013;110(30):E2762–E2771. doi:10.1073/pnas.1302156110.
[47]. White JA, Chiaramonte L, Ezzedine S, Foxall W, Hao Y, Ramirez A, McNab W. Geomechanical behavior of the reservoir and caprock system at the In Salah CO2 storage project. Proc Natl Acad Sci USA. 2014;111(24):8747–8752. doi:10.1073/pnas.1316465111.